

PRINCETON UNIVERSITY
PLASMA PHYSICS LABORATORY

THEORY DIVISION
QUARTERLY REPORT*

April 1 – June 30, 1995

*This work was supported by U.S. Department of Energy Contract No. DE-AC02-76-CHO-3073.

NOTICE

This report was prepared as an account of work sponsored by an agency of the United States Government. Neither the United States Government nor any agency thereof, nor any of their employees, makes any warranty, express or implied, or assumes any legal liability or responsibility for the accuracy, completeness, or usefulness of any information, apparatus, product, or process disclosed, or represents that its use would not infringe privately owned rights. Reference herein to any specific commercial produce, process, or service by trade name, trademark, manufacturer, or otherwise, does not necessarily constitute or imply its endorsement, recommendation, or favoring by the United States Government or any agency thereof. The views and opinions of authors expressed herein do not necessarily state or reflect those of the United States Government or any agency thereof.

This report has been reproduced directly from the best available copy.

Number of pages in this report: 14

Available to DOE and DOE contractors from the:

Office of Scientific and Technical Information

P.O. Box 62, Oak Ridge, TN 37831;

Prices available from (615) 576-8401.

Available to the public from the:

National Technical Information Service

U.S. Department of Commerce

5285 Port Royal Road, Springfield, Virginia 22161

(703) 487-4650

PPPL THEORY NEWS is a quarterly bulletin presenting condensed versions of selected research reports recently printed and distributed by the PPPL Theory Division at PPPL. Lists of printed reports and publications, external presentations at professional meetings, and recent visitors to the group are also included. Further information may be obtained by contacting the individual authors. Copies of PPPL Reports may be requested from the R & P Office at PPPL. Our address is:

Princeton Plasma Physics Laboratory

James Forrestal Campus

P.O. Box 451

Princeton, NJ 08543

Phone: (609) 243-2656

Fax: (609) 243-2662

Roscoe B. White,

Editor

Gale Stevens,

Copy Production & Layout

Contents

I	Field-aligned Coordinates for Nonlinear Simulations of Tokamak Turbulence	2
II	Theory Publication for April 1995 – June 1995	13
III	Theory Visitors for April 1995 – June 1995	14

I. Field-aligned Coordinates for Nonlinear Simulations of Tokamak Turbulence

M. A. Beer, S. C. Cowley* and G. W. Hammett

The turbulence that evolves from fine-scale instabilities (e.g. η_i , trapped electron, or resistive ballooning modes) is thought to be responsible for the anomalously large particle, momentum, and heat transport levels in tokamaks. It is therefore of great interest to simulate numerically the nonlinear evolution of these instabilities to determine the resulting fluctuation and transport levels. These instabilities are characterized by long wavelengths parallel to the magnetic field and short perpendicular wavelengths, on the order of the ion gyroradius, ρ_i . This is, of course, a consequence of the rapid communication along field lines (at the sound speed for electrostatic instabilities) and slow communication across the field lines (typically velocities across the field do not exceed the diamagnetic speed). In addition, fluctuation measurements^{1,2} in tokamaks indicate a relatively short perpendicular correlation length ($\sim 10\rho_i$), but a long parallel correlation length.³ Simulation of a full tokamak with adequate resolution of these fine perpendicular scales is somewhat beyond the presently available computational resources, since $\rho_i/a \sim 10^{-3}$ for present day large tokamaks, where a is the minor radius. (The latest full torus gyrokinetic particle simulations can now be run down to $\rho_i/a = 1/128$.⁴) However, it may be unnecessary to simulate a whole torus to reproduce small-scale, locally-driven turbulence. This paper describes a coordinate system for nonlinear simulations that resolves a much smaller volume and is therefore computationally more efficient, while still resolving the relevant small scales. The smallest possible simulation volume is a long thin flux tube that is several correlation lengths wide in both perpendicular directions (radial and poloidal), and extended along the field line, exploiting the elongated nature of the turbulence ($k_\perp \gg k_\parallel$). This approach is advantageous for fluid, gyrokinetic “Vlasov,” and particle simulations, and could eventually be compared with full torus simulations.

The fundamental idea is to use coordinates that follow field lines.⁵ With such coordinates a flux tube (a tube with a surface parallel to \mathbf{B}), which is bent by magnetic curvature and twisted by magnetic shear, is mapped into a rectangular domain. Such twisting coordinates were originally proposed by

*Dept. of Physics, UCLA

Roberts and Taylor,⁶ and Cowley *et al.*⁷ emphasized their utility for nonlinear calculations. In Ref. 8, we described the essential features of this approach, with an emphasis on slab geometry. Here we focus more on the toroidal aspects and actual details of implementation. The major problem of these field line coordinates is enforcing the periodicity constraint since the coordinates are multivalued in a torus, except at low order rational surfaces. In Ref. 7 it was emphasized that it is unlikely that the correlated volume wraps around the torus and overlaps itself. When this is true, the physical periodicity of the full torus is irrelevant, and the simplest approach is to simulate a flux tube subdomain that is several parallel correlation lengths long, just as it should be several perpendicular correlation lengths wide. As described in Ref. 5, this can be different from imposing periodicity at $\theta = \pm\pi$ as is usually suggested for the ballooning representation, which could lead to artificial correlations and modify the results.

Another advantage of field-line coordinates, in addition to the efficiency of a minimum simulation volume, is that radial periodicity can be easily implemented, thus avoiding the problems of “quasilinear flattening” and allowing self-consistent turbulence-generated “zonal” flows (flows which cause flux surfaces to rotate). The field-line coordinates are also particularly convenient for gyrofluid simulations where partially Fourier transformed quantities (in 2 of the 3 dimensions) need to be evaluated, such as $|\omega_d(\theta)| \propto |k_\theta \cos(\theta) + k_r \sin(\theta)|$.

If one wants to describe turbulence which is highly elongated along field lines and narrowly localized across field lines it is natural to introduce coordinates which are constant on field lines. A natural way to do this for any general magnetic field is to use the Clebsch representation of the magnetic field⁹ (since $\nabla \cdot \mathbf{B} = 0$):

$$\mathbf{B} = \nabla\alpha \times \nabla\psi. \quad (0.1)$$

Clearly $\mathbf{B} \cdot \nabla\alpha = \mathbf{B} \cdot \nabla\psi = 0$ so that α and ψ are constant on field lines. Thus α and ψ are natural coordinates for the flux tube. A third coordinate, z , must be defined that represents distance along the flux tube. In many applications toroidal flux surfaces are defined and it is natural to take ψ to be the poloidal flux. The choice of α is less obvious and may be optimized for a particular calculation. A further complication is that α and ψ are typically not naturally single valued and a cut must be introduced to enforce single values.⁹ This issue will be discussed extensively below. Let us imagine that

a choice of α , ψ , and z has been made and that $\alpha = \alpha(\mathbf{r})$, $\psi = \psi(\mathbf{r})$, and $z = z(\mathbf{r})$ are known functions, obtained for instance from an equilibrium code. Thus the metric coefficients for the transformation to the α, ψ, z coordinates are taken to be known.

We shall assume that the turbulence has short perpendicular correlation lengths compared to equilibrium scale lengths but a parallel correlation length on the order of the equilibrium scale lengths. Consider a flux tube simulation domain defined by $\alpha_0 - \Delta\alpha < \alpha < \alpha_0 + \Delta\alpha$, $\psi_0 - \Delta\psi < \psi < \psi_0 + \Delta\psi$, and $-z_0 < z < z_0$. This volume is chosen to be several correlation lengths in all three directions, but should be as small as possible for computational efficiency. Once the box volume is larger than several correlation lengths, the turbulence should be insensitive to the size of the box. One tests whether the box size is adequate by increasing the box size and comparing the turbulence in the different size boxes, or by measuring the correlation functions in a given box and verifying that they go to zero at the edges of the box. In this way we arrive at a minimum simulation volume.

Three spatial operators appear many times in the equations for the perturbations: $\mathbf{B} \cdot \nabla$, ∇_{\perp}^2 , and $\mathbf{B} \times \nabla\Phi \cdot \nabla$. In the field-aligned coordinates $x_i = (\alpha, \psi, z)$ these are:

$$\mathbf{B} \cdot \nabla A = (\nabla\alpha \times \nabla\psi \cdot \nabla z) \left(\frac{\partial A}{\partial z} \right)_{\alpha, \psi} = \frac{1}{J} \frac{\partial A}{\partial z}, \quad (0.2)$$

$$\nabla^2 A = \frac{1}{J} \sum_i \frac{\partial}{\partial x_i} \left[J \left(\sum_j \frac{\partial A}{\partial x_j} \nabla x_j \right) \cdot \nabla x_i \right], \quad (0.3)$$

$$\mathbf{B} \times \nabla\Phi \cdot \nabla A = \sum_{i,j} \left(\frac{\partial A}{\partial x_j} \frac{\partial \Phi}{\partial x_i} \nabla x_i \times \nabla x_j \right) \cdot \mathbf{B}, \quad (0.4)$$

where A and Φ are any scalars. Since the simulation volume is narrow in α and ψ compared to equilibrium variations, all equilibrium quantities, or gradients of equilibrium quantities when they appear in these operators, are to lowest order functions of z alone, with $\alpha = \alpha_0$ and $\psi = \psi_0$. For example, the Jacobian $J = (\nabla\alpha \times \nabla\psi \cdot \nabla z)^{-1}$ is to a good approximation constant across the box but not along the box, thus $J = J(\alpha_0, \psi_0, z)$. When A is a perturbed scalar (n , T , etc.), and Φ is the electrostatic potential, we can neglect the $\partial/\partial z$ terms in ∇_{\perp}^2 , and $\mathbf{B} \times \nabla\Phi \cdot \nabla$, since they are smaller by

k_{\parallel}/k_{\perp} . Then Eqs. (0.3,0.4) reduce to:

$$\nabla_{\perp}^2 A = |\nabla\alpha|^2 \frac{\partial^2 A}{\partial\alpha^2} + 2\nabla\alpha \cdot \nabla\psi \frac{\partial^2 A}{\partial\alpha\partial\psi} + |\nabla\psi|^2 \frac{\partial^2 A}{\partial\psi^2}, \quad (0.5)$$

$$\mathbf{B} \times \nabla\Phi \cdot \nabla A = \left(\frac{\partial A}{\partial\psi} \frac{\partial\Phi}{\partial\alpha} - \frac{\partial A}{\partial\alpha} \frac{\partial\Phi}{\partial\psi} \right) B^2. \quad (0.6)$$

Therefore, the equations to be solved in this minimum simulation volume have no explicit dependence on α or ψ , which leads to great computational simplification. The $\mathbf{E} \times \mathbf{B}$ nonlinearity takes the simple form Eq. (0.6), and all other coefficients in the equations are only functions of z .

The perpendicular boundary conditions on the perturbations at $\alpha = \alpha_0 \pm \Delta\alpha$ and $\psi = \psi_0 \pm \Delta\psi$ are taken to be periodic. If the box is more than a correlation length wide the turbulence should be insensitive to the boundary conditions, although one set of boundary conditions that is not advisable is fixed boundary conditions which prohibit energy and particle fluxes through the boundary. If fixed radial boundary conditions without sources or sinks are used, then the components of the perturbations which are constant on flux surfaces (the $m = 0, n = 0$ components, i.e. $n(\psi), T(\psi)$, where m and n are the poloidal and toroidal mode numbers) will grow to eventually cancel the driving equilibrium gradients (“quasilinear flattening”), thus turning off the turbulence. In principle, this problem can be overcome with a sufficiently large box so that the time scale to flatten the driving gradients becomes much longer than the simulation time, but periodic radial boundary conditions avoid flattening altogether and allow the use of a more efficient, smaller box. Past simulations have sometimes zeroed out the $m = 0, n = 0$ components of perturbations to avoid this flattening, but this prevents the generation of sheared zonal $\mathbf{E} \times \mathbf{B}$ flows resulting from the $m = 0, n = 0$ component of $\Phi(\psi)$, which can be an important nonlinear saturation process. Periodic radial boundary conditions allow the self-consistent evolution of $m = 0, n = 0$ perturbations such as the zonal flows.

The assumption of radial periodicity in the small flux-tube is not based on actual physical constraints, which would require simulating the full tokamak to include heating in the core, losses to the limiter or edge regions, etc.. Instead, we are assuming that the statistical properties of the fluctuations at $\psi + 2\Delta\psi$ are the same as at ψ , and that if the simulation box width $2\Delta\psi$ is larger than the radial correlation length we can assume that

they are actually identical at every instant. Periodic boundary conditions are often used in two dimensional plasma simulations or in simulations of homogeneous Navier-Stokes turbulence, but are complicated in three dimensional plasma simulations by the shear in the magnetic field. The fluctuations tend to be elongated along the direction of the magnetic field, which points in different directions at different radii. In regular coordinates this requires the use of something like the “twist-and-shift” radial boundary conditions suggested by Kotschenreuther and Wong.¹¹⁻¹³ In coordinates already aligned with the magnetic field, however, radial periodicity becomes simply $A(\psi + 2\Delta\psi, \alpha, z, t) = A(\psi, \alpha, z, t)$.

For the same reasons, we can also assume statistical periodicity in the α direction, $A(\psi, \alpha + 2\Delta\alpha, z, t) = A(\psi, \alpha, z, t)$. Since there is no explicit dependence of the operators in Eqs. (0.5,0.6) on α or ψ , we use a Fourier series in ψ and α , which also provides periodicity in those directions:

$$A(\psi, \alpha, z, t) = \sum_{j=-\infty}^{\infty} \sum_{k=-\infty}^{\infty} \hat{A}_{j,k}(z, t) e^{ij\pi(\psi-\psi_0)/\Delta\psi + ik\pi(\alpha-\alpha_0)/\Delta\alpha}. \quad (0.7)$$

The boundary conditions in the z direction are discussed in Ref. 5. Note that while each term in the Fourier series is a plane wave in α, ψ coordinates, the wavefronts in real space can be very distorted, by magnetic shear for example, measured by the parameter $\hat{s} \equiv (r_0/q_0)(\partial q/\partial r)_{r=r_0}$. Magnetic shear makes the angle between constant α and Ψ surfaces change as z changes—in real space the flux tube is then sheared and its cross-section changes from a rectangle to a parallelogram. The wavefronts of each term in the Fourier series, Eq. (0.7), also get sheared. For example the $j = 0, k \neq 0$ term has wavefronts corresponding to the constant α lines. The individual terms in the series Eq. (0.7) are therefore “twisted eddies”^{6,7} whose wavefronts twist as one moves along z .

Now let us discuss the choice of the coordinates α and ψ . As shown in Ref. 14, it is possible to choose α, ψ , and generalized “toroidal” and “poloidal” angle variables ζ and θ such that the field lines are straight in the (ζ, θ) plane and physical quantities are periodic over 2π in both variables. For the general magnetic field Eq. (0.1), we have:⁹

$$\alpha = \phi - q(\psi)\theta - \nu(\psi, \theta, \phi), \quad (0.8)$$

where $\psi = (2\pi)^{-2} \int_V d\tau \mathbf{B} \cdot \nabla \theta$ is the poloidal flux, $q(\psi) = d\psi_T/d\psi$, $\psi_T = (2\pi)^{-2} \int_V d\tau \mathbf{B} \cdot \nabla \phi$ is the toroidal flux, $d\tau$ is the volume element, and ϕ and

θ are the physical toroidal and poloidal angles, so physical quantities are periodic over 2π in ϕ and θ . The function ν is also periodic in ϕ and θ . We now introduce a new toroidal coordinate, $\zeta = \phi - \nu(\psi, \theta, \phi)$. With this choice

$$\alpha = \zeta - q(\psi)\theta, \quad (0.9)$$

and the magnetic field lines are straight in the (ζ, θ) plane, and are given by $\alpha = \text{constant}$. Further, periodicity is preserved in ζ and θ . For our parallel coordinate z we will use $z = \theta$, since this makes our description very close to the usual ballooning mode formalism. Note that z is not restricted to $-\pi < z < \pi$, as we may choose to simulate a flux tube which wraps around the torus several times in the poloidal direction, not just once.

In summary, our field-line following coordinate system is given by (ψ, α, z) , where field lines are labeled by constant ψ and α . One can think of ψ as a radial coordinate, α as a perpendicular-to-the-field coordinate, and $z = \theta$ as a parallel-to-the-field coordinate. Our notation simplifies if we introduce the following new variables:

$$x = \frac{q_0}{B_0 r_0}(\psi - \psi_0), \quad y = -\frac{r_0}{q_0}(\alpha - \alpha_0), \quad z = \theta, \quad (0.10)$$

where $q_0 = q(\psi_0)$, B_0 is the field at the magnetic axis, and r_0 is the distance from the magnetic axis to the center of the box. Then the representation of the perturbations, Eq. (0.7), becomes:

$$A(x, y, z, t) = \sum_{k_x=-\infty}^{\infty} \sum_{k_y=-\infty}^{\infty} e^{ik_x x + ik_y y} \hat{A}_{k_x, k_y}(z, t), \quad (0.11)$$

with $k_x = j\pi/\Delta x$, $k_y = -k\pi/\Delta y$, $\Delta x = q_0\Delta\psi/B_0 r_0$, and $\Delta y = r_0\Delta\alpha/q_0$. The rectangular computational box of “radial” width $2\Delta x$, and “poloidal” width $2\Delta y$, and extended along the field line, θ , is mapped onto a flux tube, as shown in Fig. 0.1, for example.

The choice of parallel boundary conditions involves a number of subtle, yet important issues.⁵ The main concept is that of a statistically-motivated periodicity, as described above for the ψ and α boundary conditions. For moderately “ballooning” turbulence we might expect parallel correlation lengths $\theta_c \sim (1 - 2)\pi$ (though it might be longer than this). The simulation box should have a length $2z_0 = 2\pi N$ in the parallel direction which is several

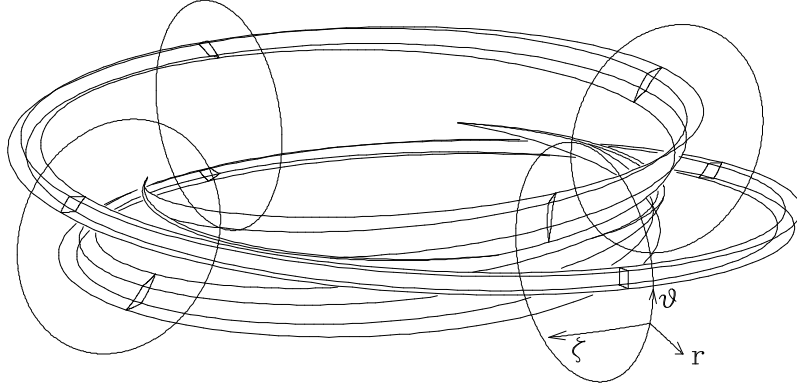


Figure 0.1: The rectangular computational domain mapped onto a flux tube in a torus, with $q_0 = 2.4$ and shear, $\hat{s} = 1.5$. The ends of this flux tube are cut off at poloidal angle $-\pi$ and π , and the sheared cross-sections of the flux tube in the poloidal plane are indicated.

times the parallel correlation length. In some cases a box length of 2π might be sufficient, but a longer box may be necessary to ensure that one end of the box is sufficiently decorrelated from the other end to avoid artificially constraining correlation effects, just as the box must be at least a few correlation lengths wide in the ψ and α directions. For the cases simulated below, parallel box lengths of at least 4π were needed for good convergence.

We have implemented this coordinate system in nonlinear gyrofluid simulations of toroidal ITG turbulence. The simulation results are presented here to describe practical computational issues and to test some of our assumptions. It is not meant to be a complete description of our gyrofluid equations or our nonlinear results, which are discussed in Ref. 10.

To test the small-scale assumption, we present two simulations, one with perpendicular dimensions ($L_x = 85\rho_i$, $L_y = 100\rho_i$), and one with double the box size ($L_x = 170\rho_i$, $L_y = 200\rho_i$). That these simulations give similar results indicates that the small flux tube may be capturing the essence of the turbulence. The physical parameters are taken from the Tokamak Fusion Test Reactor (TFTR) L-mode shot #41309: $\eta_i = 4$, $L_n/R = 0.4$, $\hat{s} = 1.5$, $q = 2.4$, $T_i = T_e$, $\rho_i = .14\text{cm}$, $L_n = 103\text{cm}$, and the computational box is centered at $r_0 = 53\text{cm}$. The box sizes then correspond to $n_0 = 10$ for the small box and $n_0 = 5$ for the large box. Both simulations use 64 grid points along the field line coordinate θ . Using 128 grid points along θ gives essentially the same results. For these runs, $N = 2$, so the physical θ domain extends from -2π to 2π . The equal length (π) extension method (for a total

extended θ domain from -3π to 3π) was used to implement the parallel boundary condition.

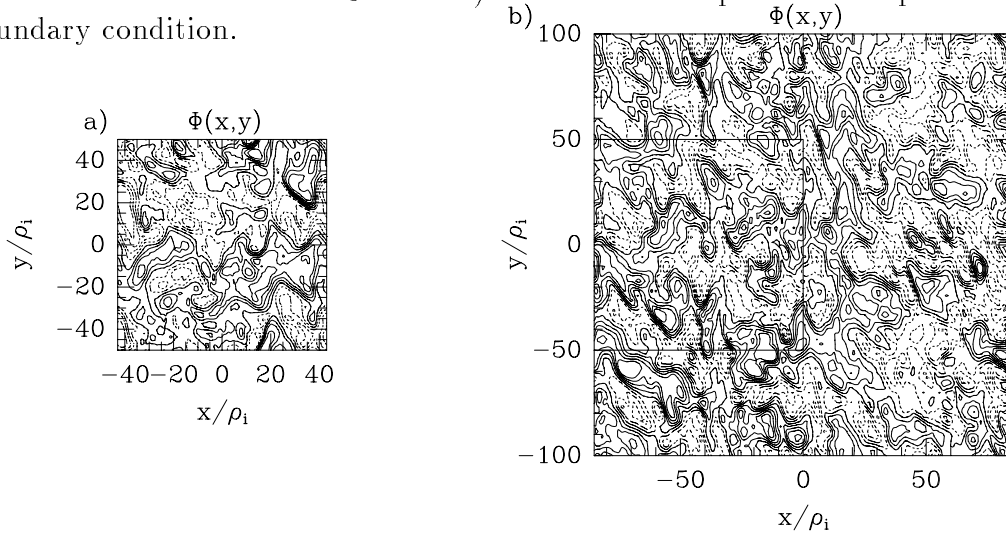


Figure 0.2: Contours of potential for a) small run, and b) large run. Doubling the perpendicular simulation domain did not change the dominant scale of the fluctuations.

Fig. 0.2 shows contours of electrostatic potential in the (x,y) plane at $\theta = 0$ (the outer midplane of the torus), for both runs at saturation. (The fluctuations on the inner midplane have roughly 1/2 the amplitude, which would be an interesting feature to look for in experiments.) It is apparent that although the box was doubled, the dominant scale didn't change. This is also evident from the spectra in Fig. 0.3, also at $\theta = 0$, where $|\Phi|^2(k_x) = \sum_{k_y} \Phi_{k_x, k_y} \Phi_{k_x, k_y}^*$, $|\Phi|^2(k_y) = \sum_{k_x} \Phi_{k_x, k_y} \Phi_{k_x, k_y}^*$, and the low resolution spectra are reduced by a factor of two to account for mode density. Although the resolution has increased, the shape and the location of the peak in the spectrum is roughly the same. These spectra are similar to BES measurements on TFTR.¹ The large $k_y = 0$ component is evidence of sheared zonal $\mathbf{E} \times \mathbf{B}$ flows,⁸ which are primarily in the poloidal direction. Though there are some small differences in the spectra, the two runs agree within statistical fluctuations on global quantities such as the volume averaged RMS fluctuation levels and transport levels: $e\Phi/T_i = 15\rho_i/L_n \simeq 0.020$ and $\chi_i = 7.4\rho_i^2 v_{ti}/L_n$, averaged from $tv_{ti}/L_n = 150 - 300$. The statistical fluctuations in χ_i at saturation are about 10% for both runs. This level of

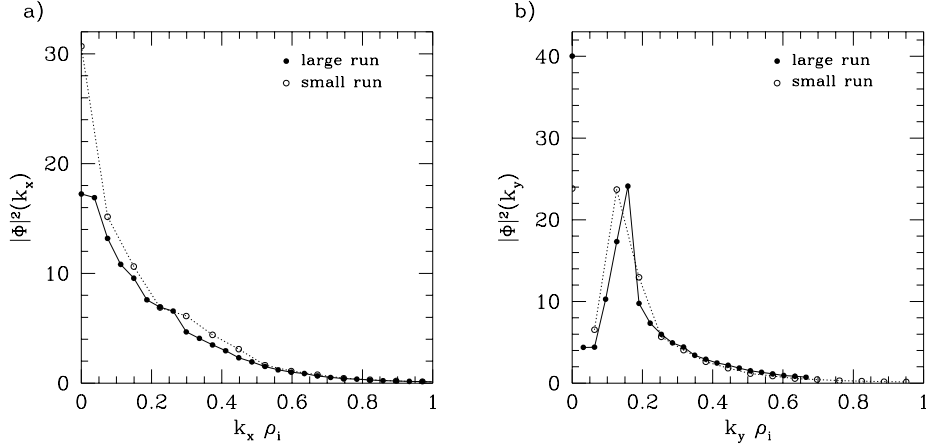


Figure 0.3: Potential spectra for both runs.

ion heat transport is near the experimentally measured $\chi_i = 8.8\rho_i^2 v_{ti}/L_n$, but these simulations ignore impurities and beams (usually a stabilizing effect), trapped electrons (destabilizing), and use our four moment model which gives lower transport than our more accurate six moment model. Nevertheless, this level of agreement is encouraging, and suggests that toroidal ITG turbulence is responsible for anomalous ion heat transport in tokamaks. The transport from these toroidal simulations is about a factor of 25 larger than sheared slab simulations for the same parameters, demonstrating the importance of toroidicity. Our toroidal simulations can be run in the sheared slab limit by taking $L_n/R \rightarrow 0$ and $q/\hat{s} \rightarrow 0$ so that $L_n/L_s = L_n\hat{s}/qR$ remains finite.

To summarize, we are simulating a rectangular domain in (x, y, z) , and using the transformation Eq. (0.10), this domain becomes a long, thin, twisting flux tube in a torus. The differential operators take the particularly useful forms Eq. (0.2-0.6), applicable to general magnetic geometry; only the metric coefficients $\nabla\alpha$, $\nabla\psi$, and ∇z need to be specified. The boundary conditions can make the perturbations periodic in θ , if $N = 1$, which makes this representation equivalent to the ballooning representation for a coarse grid in n , with spacing n_0 . However, when $n_0 > 1$, the box must be extended in θ to avoid non-physical correlations if the parallel correlation length is longer than $2\pi qR$, i.e. $\theta_c > 2\pi$. The fundamental assumptions are that the correlation lengths (both parallel and perpendicular) are smaller than the box size, that the equilibrium gradients vary slowly across the small perpendicular extent of the box, and that the turbulence is local, i.e. driven only by

the equilibrium gradients within the box. For typical tokamak parameters, our reduced simulation volume can represent large computational savings.

References

- ¹R. J. Fonck, G. Cosby, R. D. Durst, S. F. Paul, N. Bretz, S. Scott, E. Synakowski, and G. Taylor, *Phys. Rev. Lett.* **70**, 3736 (1993).
- ²E. Mazzucato and R. Nazikian, *Phys. Rev. Lett.* **71**, 1840 (1993).
- ³S. Zweben and S. S. Medley, *Phys. Fluids B* **1**, 2058 (1989).
- ⁴S. E. Parker, J. C. Cummings, W. W. Lee, and H. E. Mynick, in *Proceedings of the Joint Varenna-Lausanne International Workshop on Theory of Fusion Plasmas*, (Societa Italiana di Fisica, Bologna, 1994).
- ⁵M. A. Beer and S. C. Cowley and G. W. Hammett, to appear in *Phys. Plasmas* (1995).
- ⁶K. V. Roberts and J. B. Taylor, *Phys. Fluids* **8**, 315 (1965).
- ⁷S. C. Cowley, R. M. Kulsrud, and R. Sudan, *Phys. Fluids B* **3**, 2767 (1991).
- ⁸G. W. Hammett, M. A. Beer, W. Dorland, S. C. Cowley, and S. A. Smith, *Plasma Phys. Controlled Fusion* **35**, 973 (1993).
- ⁹M. D. Kruskal and R. M. Kulsrud, *Phys. Fluids* **1**, 265 (1958).
- ¹⁰M. A. Beer, Ph.D. Thesis, Princeton University (1994).
- ¹¹W. Dorland, G. W. Hammett, T. S. Hahm, and M. A. Beer, in *U. S.-Japan Workshop on Ion Temperature Gradient Driven Turbulent Transport*, edited by W. Horton, M. Wakatani, and A. Wootton, (American Institute of Physics, New York, 1993), p. 344.
- ¹²M. Kotschenreuther and H. V. Wong, private communication (1991).
- ¹³A. M. Dimits, *Phys. Rev. E* **48**, 4070 (1993).
- ¹⁴J. M. Greene and J. L. Johnson, *Phys. Fluids* **5**, 510 (1962).

II. Theory Publication for April 1995 – June 1995

Gorelenkov, N. and C. Z. Cheng, *Alfvén Cyclotron Instability and Ion Cyclotron Emission*, IAEA Technical Committee Meeting and Joint US-Japan Workshop on Alpha Particles in Fusion Research, Princeton University, Plasma Physics Laboratory Report PPPL-3114. Submitted to Nuclear Fusion.

Hahm, T. S. and K. H. Burrell, *$\mathbf{E} \times \mathbf{B}$ Flow Shear Effects on Radial Correlation Length of Turbulence and Gyroradius Scaling of Confinement*, Princeton University, Plasma Physics Laboratory Report PPPL-3126. Submitted to Physics of Plasmas.

Naitou, H., K. Tsuda, W. W. Lee, and R. D. Sydora, *Gyrokinetic Simulation of Internal Kink Modes*, Princeton University, Plasma Physics Laboratory Report PPPL-3101. Submitted to Physics of Plasmas.

Lee, W. W. and R. Santoro, *Gyrokinetic Simulation of Isotope Scaling in Tokamak Plasmas*, Princeton University, Plasma Physics Laboratory Report PPPL-3123. Submitted to Phys. Rev. Lett.

Park, W., E. Fredrickson, A. Janos, J. Manickam, and W. M. Tang, *High- β Disruptions in Tokamaks*, Princeton University, Plasma Physics Laboratory Report PPPL-3104. Submitted to Nuclear Fusion.

Wu, Y., R. B. White, Y. Chen, and M. N. Rosenbluth, *Nonlinear Evolution of the Alpha Particle Driven Toroidicity-Induced Alfvén Eigenmode*, Princeton University, Plasma Physics Laboratory Report PPPL-3103. Submitted to Physics of Plasmas.

White, R. B., Y. Wu, Y. Chen, E. Fredrickson, D. Darrow, M. Zarnstorff, R. Wilson, S. Zweben, K. Hill, G. Fu, and M. N. Rosenbluth, *Nonlinear Analysis of the Toroidicity-Induced Alfvén Eigenmode*, IAEA Technical Committee Meeting and Joint US-Japan Workshop on Alpha Particles in Fusion Research. Submitted to Nuclear Fusion.

Rogers, B. and L. Zakharov, *Nonlinear ω_* -Stabilization of the $m = 1$ Mode in Tokamaks*, Princeton University Plasma Physics Laboratory Report PPPL-3125. Submitted to Physics of Plasmas

III. Theory Visitors for April 1995 – June 1995

Boozer, A., Columbia University, April 27.

Chen, L., University of California, Irvine, April 10-16, and May 29-June 4.

Dremin, I., Lebedev Institute, Moscow, May 18-19.

Evrard, M., Plasma Physics Laboratory, Royal Military Academy, Brussels, Belgium, May 22-25.

Fitzpatrick, R., Institute for Fusion Studies, University of Texas at Austin, June 11-24.

Fivaz, M., Center for Plasma Physics Research, Lausanne, Switzerland, May 1-5.

Kepner, J., Princeton University, DoE Computational Graduate Fellowship Summer Intern, June 12-September 1, 1995.

Kritz, A., Lehigh University, approximately 1 day/month April - June.

Merkel, P., Max-Planck Institut fuer Plasmaphysik, Germany, April 6-28.

Pastukhov, V., Kurchatov Institute of Atomic Energy, Russian Federation, June 13-16.

Pigarov, A., Kurchatov Institute of Atomic Energy, Russian Federation, May 15, 1995 to May 15, 1996.

Salas, A., CIEMAT, Madrid, Spain, June 20-August 20.

Shafranov, V., Kurchatov Institute of Atomic Energy, Russian Federation, June 13-16.

Solano, E., Fusion Research Center, University of Texas at Austin, June 5-9.

Summer Science Education Program Visitors

Summer Research Program for Under Represented Groups

Huang, T. S., Prairie View A & M University, June 2-August 18.

Sen, A., Mt. Holyoke College, June 2-August 18.

Smith, I., Prairie View A & M University, June 2-August 18.

Storr, K., Prairie View A & M University, June 2-August 18.

Upshaw, S., Hampton University, June 2-August 18.

Yu, X., Prairie View A & M University, June 2-August 18.

National Undergraduate Fellowship Program

Chen, L., Duke University, June 19-August 25.

Fu, Q., Hamilton College, June 19-August 25.

Strasburg, S., Benedictine College, June 19-August 25.